Viscoelastic behavior of periodontal ligament: stresses relaxation during continuing translational displacement of tooth root

S. Bosiakov, G. Mikhasev and S. Rogosin

Abstract. Understanding of viscoelastic response of a periodontal membrane under the action of short-term and long-term loadings is important for many orthodontic problems. A new analytic model describing behavior of the viscoelastic periodontal ligament after the tooth root translational displacement is suggested. In the model, a tooth root and alveolar bone are assumed to be a rigid bodies. The system of differential equations for the plane-strain state of the viscoelastic periodontal ligament are used as the governing equations. The boundary conditions corresponding to the initial small displacement of the root and fixed outer surface of the periodontal ligament in the dental alveolus were employed. A solution is found numerically for fractional viscoelasticity model in assumption that the stresses relaxation in the periodontal ligament after the continuing displacement of the tooth root occurs within about five hours. A character of stresses distribution in the ligament over time caused by the tooth root translational displacement is evaluated. Effect of Poisson's ratio on the stresses in the viscoelastic periodontal ligament is considered. The obtained results can be used for simulation of the bone remodelling process during orthodontic treatment and for assessment of optimal conditions of the orthodontic load application.

Mathematics Subject Classification (2010). 74L15; 35Q74; 92C10.

Keywords. Viscoelastic periodontal ligament, translational displacement, root of the tooth, stress relaxation.

1. Introduction

A tooth root is attached to alveolar bone by a periodontal ligament (PDL), a soft connective tissue consisting of collagen fibres and a matrix phase with nerve endings and blood vessels [1, 2]. Because of the low stiffness the PDL has a central role in the tooth mobility [3] and acts basically as a physiological mechanism responsible for the teeth movements and teeth reaction to loading

[4, 5, 6]. The long-term force action on the tooth is characterized of its nearly instantaneous displacement in the PDL with a subsequent relaxation of the stresses during five hours of the load action [7]. At that the PDL reveals the viscoelastic and time-dependent properties [8, 9, 10, 11, 20, 13].

An analytical model of the initial (instantaneous) translational displacements of the tooth root in the PDL under the static load action has been proposed in study [14]. This model has several advantages compared with other known analytical models [15, 16]. These advantages are the possibility to use arbitrary elastic constants for the PDL tissue and assess stresses in the PDL without simplifying assumptions. The static model developed in paper [14] permits also to evaluate the stress-strain state of the PDL throughout its thickness. The direct and logical evolution of this model seems to be taking into account the viscoelastic properties of the periodontal ligament. Such model allowing for both the stress relaxation and slow displacement of teeth could be employed in the real clinical practice for the bone reconstruction during the orthodontic treatment.

Analytical modelling of the PDL viscoelastic response under the tooth long-term loading were carried out in references [17, 18, 19]. In particular, in [17], a nonlinear viscoelastic constitutive model was adopted to describe the relaxation phenomena in the PDL that consistent with experimental data about dependence of relaxation rate on the level of applied strain. The proposed model allows with sufficient accuracy to evaluate the PDL behavior under the high rate loading and large strains of the PDL tissue. At the same time, modelling of the tooth roots motions in the viscoelastic PDL was not carried out in [17]. The mathematical model with single degree of freedom to define the initial posterior tooth displacement in the viscoelastic PDL associated with functioning interproximal contacts was developed in paper[18]. This model is described by ordinary differential equations with constant coefficients and allows to simulate the short-term movements of the teeth at the occurrence of the contact between the adjacent teeth. In [19] a mathematical model for description of experimentally observed viscoelastic and time-dependent behaviours of the PDL was developed. The analysis is focused on the evolution of translational displacements of the tooth root in the PDL under the vertical load (intrusion). The calculated tooth-root displacement with time at a constant load allowed comparing the behaviour of the viscoelastic model with the fractional exponential kernel with that of the known nonlinear viscoelastic model of the tooth-root movement developed in the studies [20, 18]. Proposed in [19] model allows generalization of the known analytical models of the viscoelastic PDL by introduction of the instantaneous and relaxed elastic moduli, as well as the fractional parameter. The advantage of this model is in the use of the fractional parameter improving the description of various pathological processes and age-related changes in the PDL. The fractional parameter makes it possible to take into

account different behaviours of the periodontal tissue under short- and long-term loads. For instance, it allows assessing the change in the time interval of a transition phase for a given maximum displacement.

The aim of this study is to develop a 2-D analytical model of the PDL viscoelastic response which would permit to predict the stress-strain state of the PDL characterized by the phenomena of relaxation and the continuing translational movement of the tooth root as well. A 2-D model is quite sufficient to describe the PDL behavior during the translational movement of the tooth root, with the exception of the small PDL regions near the root apex and the alveolar crest. This is due to the conclusions of studies [15, 16], that the vertical displacements of the PDL points are very small and can be neglected, with the exception displacements of the PDL points at the regions near the apex and the alveolar crest.

2. Viscoelastic model of the PDL

It is assumed that at the initial time moment the tooth root is shifted horizontally at a distance u_0. The cross-section of the tooth root is circular in the any plane perpendicular to the longitudinal axis of the tooth. The tooth root is considered as the rigid body compared to the PDL tissue [21]. Positions of the root section before and after the displacement, as well as the geometric dimensions of the root cross-section are shown in Figure 1.

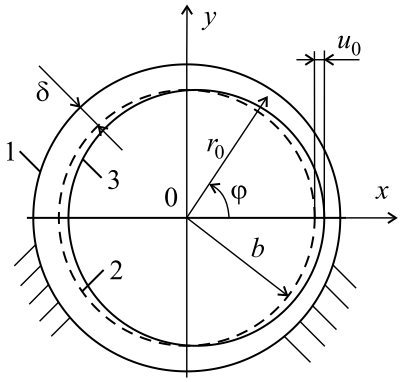

FIGURE 1. Positions of tooth root in sectional plane before and after displacement on the distance u_0: 1 – outer contour of the PDL fixed on dental alveolus surface; 2 – position of cross-section of tooth root before load action; 3 – position of cross-section of tooth root after load action; u_0 is the tooth root displacement in the x-direction; r_0 is the radial coordinate, φ is the polar angle.

In the polar coordinate system r_0, φ (see Figure 1), the constitutive equations for the viscoelastic PDL are taken in the form:

$$\begin{aligned}
\sigma_{rr}(r_0,\varphi,t) &= \lambda\left(e_{\varphi\varphi}(r_0,\varphi,t) - \int_0^t K(t-\tau)e_{\varphi\varphi}(r_0,\varphi,t)d\tau\right) + \\
&\quad (\lambda+2\mu)\left(e_{rr}(r_0,\varphi,t) - \int_0^t K(t-\tau)e_{rr}(r_0,\varphi,t)d\tau\right) + \\
\sigma_{r\varphi}(r_0,\varphi,t) &= 2\mu\left(e_{r\varphi}(r_0,\varphi,t) - \int_0^t K(t-\tau)e_{r\varphi}(r_0,\varphi,t)d\tau\right), \qquad (2.1)\\
\sigma_{\varphi\varphi}(r,\varphi,t) &= \lambda\left(e_{rr}(r_0,\varphi,t) - \int_0^t K(t-\tau)e_{rr}(r,\varphi,t)d\tau\right) + \\
&\quad (\lambda+2\mu)\left(e_{\varphi\varphi}(r_0,\varphi,t) - \int_0^t K(t-\tau)e_{\varphi\varphi}(r_0,\varphi,t)d\tau\right),
\end{aligned}$$

where $\sigma_{rr}, \sigma_{r\varphi}, \sigma_{\varphi\varphi}$ and $e_{rr}, e_{r\varphi}, e_{\varphi\varphi}$ are the components of the stress and strain tensors, respectively; $\lambda = \frac{E_0\nu}{(1-2\nu)(1+\nu)}$ and $\mu = \frac{E_0}{2(1+\nu)}$ are Lame parameters; E_0 and ν are the instantaneous modulus elasticity and Poisson's ratio of the PDL (ν=const); $K(t)$ is the relaxation kernel for the normal and shear components of stresses; $u_r(r_0,\varphi,t)$, $u_\varphi(r_0,\varphi,t)$ are the radial and circular displacements of the PDL points, respectively.

The strain tensor components are

$$\begin{aligned}
e_{rr}(r_0,\varphi,t) &= \frac{\partial u_r(r_0,\varphi,t)}{\partial r},\\
e_{\varphi\varphi}(r_0,\varphi,t) &= \frac{1}{r_0}\left(\frac{\partial u_\varphi(r_0,\varphi,t)}{\partial\varphi} + u_r(r_0,\varphi,t)\right), \qquad (2.2)\\
e_{r\varphi} &= \frac{1}{2}\left(\frac{1}{r_0}\frac{\partial u_r(r_0,\varphi,t)}{\partial\varphi} + \frac{\partial u_\varphi(r_0,\varphi,t)}{\partial r} - \frac{u_\varphi(r_0,\varphi,t)}{r_0}\right).
\end{aligned}$$

Equations (2.1) and (2.2) consistently employ in the equations of the PDL motion

$$\begin{aligned}
\frac{\partial\sigma_{rr}}{\partial r_0} + \frac{1}{r_0}\frac{\partial\sigma_{r\varphi}}{\partial\varphi} + \frac{\sigma_{rr}-\sigma_{\varphi\varphi}}{r_0} &= \rho\frac{\partial^2 u_r(r_0,\varphi,t)}{\partial t^2},\\
\frac{1}{r_0}\frac{\partial\sigma_{\varphi\varphi}}{\partial\varphi} + \frac{\partial\sigma_{r\varphi}}{\partial r_0} + \frac{2\sigma_{r\varphi}}{r_0} &= \rho\frac{\partial^2 u_\varphi(r_0,\varphi,t)}{\partial t^2},
\end{aligned} \qquad (2.3)$$

where ρ is the density of the PDL tissue.

The substitution of (2.1) and (2.2) into Eqs. (2.3) results in the following system of integro-differential equations:

$$\begin{aligned}
&\left(r_0\frac{\partial^2}{\partial r_0^2}+\frac{\partial}{\partial r_0}-\frac{1}{r_0}+\frac{\mu}{\lambda+2\mu}\frac{1}{r_0}\frac{\partial^2}{\partial\varphi^2}\right)\\
&\left(u_r(r_0,\varphi,t)-\int_0^t K(t-\tau)u_r(r_0,\varphi,t)d\tau\right)+\\
&+\left(\frac{\lambda+\mu}{\lambda+2\mu}\frac{\partial^2}{\partial\varphi\partial r_0}-\frac{\lambda+3\mu}{\lambda+2\mu}\frac{1}{r_0}\frac{\partial}{\partial\varphi}\right)\\
&\left(u_\varphi(r_0,\varphi,t)-\int_0^t K(t-\tau)u_\varphi(r_0,\varphi,t)d\tau\right)=\rho\frac{\partial^2u_r(r_0,\varphi,t)}{\partial t^2},\\
&\left(\frac{\lambda+\mu}{\lambda+2\mu}\frac{\partial^2}{\partial\varphi\partial r_0}+\frac{\lambda+3\mu}{\lambda+2\mu}\frac{1}{r_0}\frac{\partial}{\partial\varphi}\right)\\
&\left(u_r(r_0,\varphi,t)-\int_0^t K(t-\tau)u_r(r_0,\varphi,t)d\tau\right)+\\
&+\left(\frac{\mu r_0}{\lambda+2\mu}\frac{\partial^2}{\partial r_0^2}+\frac{\mu}{\lambda+2\mu}\frac{\partial}{\partial r_0}-\frac{\mu}{\lambda+2\mu}\frac{1}{r_0}+\frac{1}{r_0}\frac{\partial^2}{\partial\varphi^2}\right)\\
&\left(u_\varphi(r_0,\varphi,t)-\int_0^t K(t-\tau)u_\varphi(r_0,\varphi,t)d\tau\right)=\rho\frac{\partial^2u_\varphi(r_0,\varphi,t)}{\partial t^2}.
\end{aligned}$$

The above equations may be rewritten in the dimensionless form:

$$\begin{aligned}
&a_{11}\left(u(r,\varphi,t)-\int_0^t K(t-\tau)u(r,\varphi,t)d\tau\right)+\\
&a_{12}\left(v(r,\varphi,t)-\int_0^t K(t-\tau)v(r,\varphi,t)d\tau\right)=\varepsilon\frac{\partial^2u(r,\varphi,t)}{\partial t^2},\\
&a_{21}\left(u(r,\varphi,t)-\int_0^t K(t-\tau)u(r,\varphi,t)d\tau\right)+\\
&a_{22}\left(v(r,\varphi,t)-\int_0^t K(t-\tau)v(r,\varphi,t)d\tau\right)=\varepsilon\frac{\partial^2v(r,\varphi,t)}{\partial t^2},
\end{aligned}\tag{2.4}$$

where

$$a_{11} = r(1-\nu)\frac{\partial^2}{\partial r^2} + (1-\nu)\frac{\partial}{\partial r} - \frac{1-\nu}{r} + \frac{1-2\nu}{2}\frac{1}{r}\frac{\partial^2}{\partial \varphi^2},$$
$$a_{12} = \frac{1}{2}\frac{\partial^2}{\partial \varphi \partial r} - \frac{3-4\nu}{2}\frac{1}{r}\frac{\partial}{\partial \varphi}, a_{21} = \frac{1}{2}\frac{\partial^2}{\partial \varphi \partial r} + \frac{3-4\nu}{2}\frac{1}{r}\frac{\partial}{\partial \varphi},$$
$$a_{22} = \frac{(1-2\nu)r}{2}\frac{\partial^2}{\partial r^2} + \frac{1-2\nu}{2}\frac{\partial}{\partial r} - \frac{1-2\nu}{r} + \frac{1-\nu}{r}\frac{\partial^2}{\partial \varphi^2}.$$

Here, $u(r,\varphi,t) = \frac{u_r(r,\varphi,t)}{h}$, $v(r,\varphi,t) = \frac{u_\varphi(r,\varphi,t)}{h}$ are the dimensionless displacements, $r = \frac{r_0}{h}$ is the dimensionless radial coordinate, h is the tooth root height, $\varepsilon = \frac{\rho h^2}{E_0 t_0^2}(1+\nu)(1-2\nu)$ is a dimensionless parameter, and t_0 is the characteristic time.

The time of the stress relaxation in the PDL is obviously about five hours [7]. In our study, the characteristic time is assumed as $t_0 = 1$ h. In this case a dimensionless parameter ε turns out to bee very small, and equations (2.4) become the singularly perturbed ones with respect to the inertia terms. When $\varepsilon \to 0$, equations (2.4) degenerates into the stationary ones studied in reference [14].

It is assumed that during the tooth root translational movement in the PDL, the required displacements can be represented as products of independent functions

$$u(r,\varphi,t) = u_1(r,t)\cos(\varphi), \quad v(r,\varphi,t) = v_1(r,t)\sin(\varphi). \tag{2.5}$$

Inserting (2.5) into equations (2.4) yields the following system of equations:

$$\begin{gathered} A_{11}\left(u_1(r,t) - \int_0^t K(t-\tau)u_1(r,t)d\tau\right) + \\ A_{12}\left(v_1(r,t) - \int_0^t K(t-\tau)v_1(r,t)d\tau\right) = \varepsilon\frac{\partial^2 u_1(r,t)}{\partial t^2}, \\ A_{21}\left(u_1(r,t) - \int_0^t K(t-\tau)u_1(r,t)d\tau\right) + \\ A_{22}\left(v_1(r,t) - \int_0^t K(t-\tau)v_1(r,t)d\tau\right) = \varepsilon\frac{\partial^2 v_1(r,t)}{\partial t^2}. \end{gathered} \tag{2.6}$$

with the differential operators A_{ij} defined as

$$A_{11} = r(1-\nu)\frac{\partial^2}{\partial r^2} + (1-\nu)\frac{\partial}{\partial r} - \frac{3-4\nu}{2r},$$
$$A_{12} = \frac{1}{2}\frac{\partial}{\partial r} - \frac{3-4\nu}{2}\frac{1}{r}, A_{21} = -\frac{1}{2}\frac{\partial}{\partial r} - \frac{3-4\nu}{2}\frac{1}{r},$$
$$A_{22} = \frac{(1-2\nu)r}{2}\frac{\partial^2}{\partial r^2} + \frac{1-2\nu}{2}\frac{\partial}{\partial r} - \frac{3-4\nu}{2r}.$$

Let us apply the Laplace transform to equations (2.6) with the initial conditions

$$u_1(r,0) = u_2(r),\ v_1(r,0) = v_2(r),$$
$$\left.\frac{\partial u_1(r,t)}{\partial t}\right|_{t=0} = 0,\ \left.\frac{\partial v_1(r,t)}{\partial t}\right|_{t=0} = 0, \tag{2.7}$$

where $u_2(r)$ and $v_2(r)$ are the initial displacements of the PDL points emerging after the instantaneous shift of the tooth root by the distance u_0 (see paper [14]).

As a result, one obtains the system of differential equations

$$\begin{aligned} B_{10}\left(B_{11} + B_{12}\frac{\partial}{\partial r} + B_{13}\frac{\partial^2}{\partial r^2}\right)u_1^\star(r,p) + \\ \left(B_{14} + B_{15}\frac{\partial}{\partial r}\right)v_1^\star(r,p) = 0, \\ B_{20}\left(B_{21} + B_{22}\frac{\partial}{\partial r} + B_{23}\frac{\partial^2}{\partial r^2}\right)v_1^\star(r,p) + \\ \left(B_{24} + B_{25}\frac{\partial}{\partial r}\right)u_1^\star(r,p) = 0, \end{aligned} \tag{2.8}$$

with respect to the functions $u_1^\star(r,p)$, $v_1^\star(r,p)$ being the Laplace transforms of $u_1(r,t)$, $v_1(r,t)$, respectively. Here

$$B_{10} = -p\varepsilon u_1(r), B_{11} = \varepsilon p^2 - \frac{f(p)(3-4\nu)}{2r^2},$$
$$B_{12} = \frac{f(p)(1-\nu)}{r}, B_{13} = f(p)(1-\nu), B_{14} = -\frac{f(p)(3-4\nu)}{2r^2},$$
$$B_{15} = \frac{f(p)}{2r}, B_{20} = -p\varepsilon v_1(r), B_{21} = \varepsilon p^2 - \frac{f(p)(3-4\nu)}{2r^2},$$
$$B_{22} = \frac{f(p)(1-2\nu)}{2r}, B_{23} = \frac{f(p)(1-2\nu)}{2}, B_{24} = -\frac{f(p)(3-4\nu)}{2r^2},$$
$$B_{25} = -\frac{f(p)}{2r}, f(p) = -1 + K^\star(p), \quad K^\star = \int_0^\infty K(t)\exp(-pt)\mathrm{d}t.$$

It should be noted that equations (2.8) turn out to be regularly perturbed by a small parameter ε. Their solution may be sought in the form of

asymptotic series:

$$u_1^\star(r,p)=\sum_{k=1}^{\infty}u_{0k}^\star(r,p)\varepsilon^{k-1},\ v_1^\star(r,p)=\sum_{k=1}^{\infty}v_{0k}^\star(r,p)\varepsilon^{k-1}. \tag{2.9}$$

Overview of the ranges of Poisson's ratios and elastic moduli for the PDL indicates that their lowest values are 0.28 and 0.01 MPa, respectively [1, 22, 23, 24]. The density of the PDL tissue is equal to 1.06 g/cm^3 [28]. The tooth root height is assumed to be 13.0 mm, the thickness of the PDL along the normal to the inner surface is about 0.229 mm [15]. Commonly used the elastic constants are $E_0 = 680$ kPa and $\nu = 0.49$ [15, 25, 26, 16]. For the geometric and time-material constants mentioned above, the small parameter ε amounts approximately to $6.06{\cdot}10^{-16}$.

The substitution of expansions (2.9) into equations (2.8) results in a sequence of differential equations for functions $u_{0k}^\star, v_{0k}^\star$. Let us consider here only the first two approximations. They produce the following two systems:

$$\begin{aligned}C_{11}u_{01}^\star(r,p)+C_{12}v_{01}^\star(r,p)=0,\\ C_{21}u_{01}^\star(r,p)+C_{22}v_{01}^\star(r,p)=0,\end{aligned} \tag{2.10}$$

and

$$\begin{aligned}-p(u_2(r)-pu_{01}^\star(r,p))+C_{11}u_{02}^\star(r,p)+C_{12}v_{02}^\star(r,p)=0,\\ -p(v_2(r)-pv_{01}^\star(r,p))+C_{21}u_{02}^\star(r,p)+C_{22}v_{02}^\star(r,p)=0,\end{aligned} \tag{2.11}$$

where

$$C_{11}=-\frac{3-4\nu}{2r^2}+\frac{1-\nu}{r}\frac{\partial}{\partial r}+(1-\nu)\frac{\partial^2}{\partial r^2},C_{12}=\frac{1}{2r}\left(-\frac{3-4\nu}{r}+\frac{\partial}{\partial r}\right),$$
$$C_{21}=\frac{1}{2r}\left(-\frac{3-4\nu}{r}-\frac{\partial}{\partial r}\right),C_{22}=-\frac{3-4\nu}{2r^2}+\frac{1-2\nu}{2r}\frac{\partial}{\partial r}+\frac{1-2\nu}{2}\frac{\partial^2}{\partial r^2}$$

are the differential operators.

The solution of equations (2.10) is the following [14]:

$$\begin{aligned}u_{01}^\star(r,p)=c_{01}(1-4\nu)r^2+\frac{c_{02}}{r}-\frac{c_{03}}{2(3-4\nu)}+c_{03}\ln(r)+c_{04},\\ v_{01}^\star(r,p)=c_{01}(5-4\nu)r^2+\frac{c_{02}}{r}-\frac{c_{03}}{2(3-4\nu)}-c_{03}\ln(r)-c_{04},\end{aligned} \tag{2.12}$$

where c_{0k} are unknown constants, $k=\overline{1,4}$. Taking into account the initial displacements $u_2(r)$ and $v_2(r)$, the solution of equations (2.11) can be represented in the form of functions

$$\begin{aligned}u_{02}^\star(r,p)=b_{13}r^4+b_{23}r^2\ln(r)+b_{33}+b_{43}r^2,\\ v_{02}^\star(r,p)=f_{13}r^4+f_{23}r^2\ln(r)+f_{33}+f_{43}r^2\end{aligned} \tag{2.13}$$

with the coefficients

$$b_{13} = -\frac{p(pc_{01} - p_{01})(1 - 12\nu + 16\nu^2)}{24(1 - 3\nu + 2\nu^2)f^\star(p)}, f_{13} = -\frac{p(pc_{01} - p_{01})(19 - 36\nu + 16\nu^2)}{24(1 - 3\nu + 2\nu^2)f^\star(p)},$$

$$b_{33} = f_{33} = \frac{p(pc_{02} - p_{02})}{(3 - 4\nu)f^\star(p)}, b_{23} = -\frac{p(c_{03} - p_{03})(7 - 20\nu + 16\nu^2)}{8(3 - 13\nu + 18\nu^2 - 8\nu^3)f^\star(p)},$$

$$f_{23} = \frac{2p(pc_{03} - p_{03}) - b_{23}(21 - 52\nu + 32\nu^2)f^\star(p)}{(15 - 44\nu + 32\nu^2)f^\star(p)},$$

$$b_{43} = f_{43} = \frac{p\left((pc_{03} - p_{03})(17 - 48\nu + 32\nu^2) - 16(pc_{04} - p_{04})(1 - 3\nu + 2\nu^2)\right)}{32(1 - 3\nu + 2\nu^2)f^\star(p)}.$$

Unknown constants c_{0k}, $k = \overline{1,4}$ are determined numerically via the inverse Laplace transform of the solutions of equations (2.9) and functions (2.12), (2.13) as well taking into account the following boundary conditions:

$$u_1(b,0) = u_0, \quad v_1(b,0) = u_0, \quad u_1(b_1,0) = 0, \quad v_1(b,0) = 0. \tag{2.14}$$

The inverse Laplace transformation was performed using the geometric dimensions b and b_1 of the cross-section corresponding to the tooth root in the shape of a circular paraboloid; the radius of the inner tooth surface at the alveolar crest level was 3.9 mm [15]. The viscoelastic properties of the PDL are described by model with fractional derivatives [29]. It was introduced by Rabotnov in the following form [30, 31]:

$$\mathcal{E}_\gamma\left(-\frac{t}{\tau_\varepsilon}\right) = \frac{t^{\gamma-1}}{\tau_\varepsilon^\gamma}\sum_{n=0}^{\infty}(-1)^n\frac{(t/\tau_\varepsilon)^{\gamma n}}{\Gamma[\gamma(n+1)]},$$

where $0 < \gamma < 1$ is the fractional parameter. Note that the Rabotnov's function is a special case of the classical Mittag-Leffler function widely used in fractional models (see [32, 33]). The parameter γ and retardation time τ_s for the model of viscoelasticity model with fractional exponential kernel were taken as 0.3 and 550 s, respectively [19]. In accordance with study [7], it was suggested that the stresses relaxation in the PDL after starting the load action (and subsequent instantaneous displacement of the tooth root in the PDL) occurred within about five hours.

2.1. Evolution of stresses in the PDL

Patterns of the radial normal component $\sigma_{rr}(r, \varphi, t_k)$ of stresses in the PDL for points of time $t_1 = 0.25$ h, $t_2 = 1$ h, $t_3 = 2$ h and $t_4 = 5$ h are shown in Figure 2 ($-\pi/2 \le \varphi \le \pi/2$). Elastic constants for the PDL were taken to be equal to $E = 680$ kPa and $\nu = 0.49$ [15, 25, 26, 16]; the height of the tooth root was 13.0 mm, thickness of the PDL along normal to its inner surface was 0.229 mm [15]. The radii of the inner and outer surface of the PDL corresponded to the middle third of the tooth root in the form of a circular paraboloid (radius of the tooth cross-section at the alveolar crest level was equal to 3.9 mm). The load applied to the tooth was 1 N; due to this load, the instantaneous dimensionless initial displacement was $u_0 = 18.15 \cdot 10^{-6}$ [14].

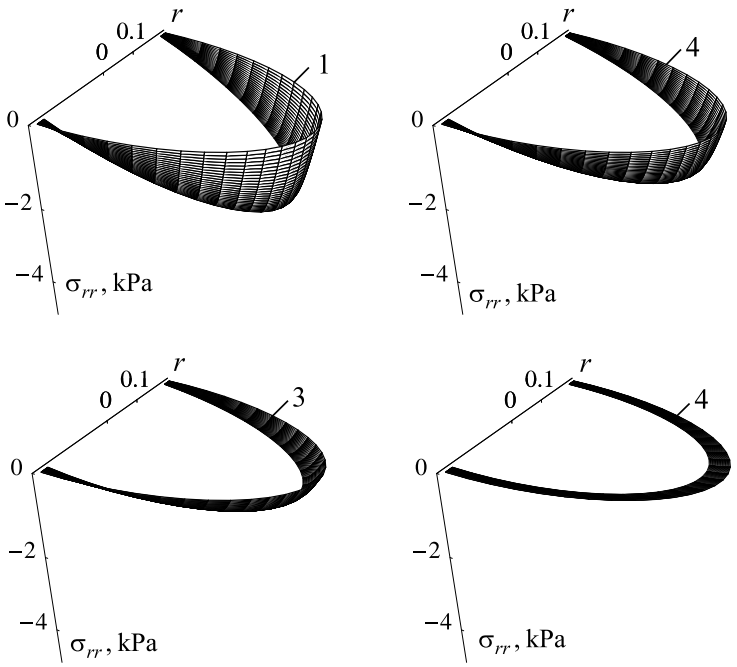

FIGURE 2. Patterns of the radial normal components σ_{rr} of stresses in the PDL for different point of time: 1 – $t = 0.25$ h; 2 – $t = 1$ h; 3 – $t = 2$ h; 4 – $t = 5$ h.

It is seen from Figure 2 that the radial stresses throughout the PDL thickness change significantly. For any point of time and for the fixed radial coordinate, the circular stresses at the PDL outer surface almost are equal to zero. The stresses pattern (see Figure 2) corresponds to the compressive region ($\pi/2 \le \varphi \le 3\pi/2$) of the PDL located in the direction of the tooth root movement. The patterns of the tensile radial stresses with respect to the coordinate origin are symmetric to the corresponding patterns of the compressive stresses for the same point of time. The maximum and minimum radial stresses occure on the PDL inner surface at $\varphi = \pi$ and $\varphi = 0$, respectively. The patterns of the circular component $\sigma_{\varphi\varphi}$ of stresses on the radial and circular coordinates for various points of time are similar to the patterns shown in Figure 2.

Figure 3 shows the radial component σ_{rr} of stresses versus time for a point on the PDL inner surface at $\varphi = 0$ for different initial displacements. The geometric and material constants as well as the conditions of the load application were the same.

Figure 3 depicts that the larger the applied load is, the longer period of time for the total relaxation of stresses in the PDL is required.

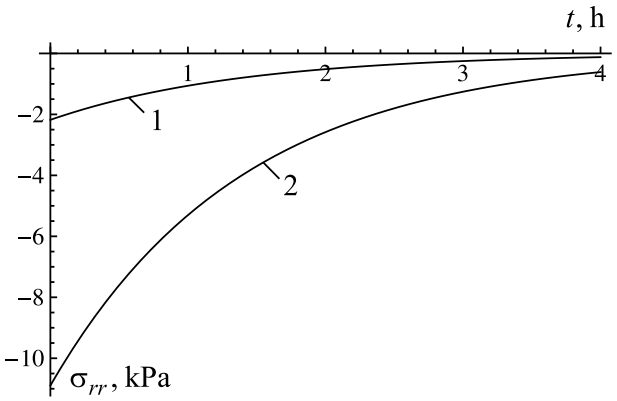

FIGURE 3. Radial component $\sigma_{rr}(b, 0, t)$ of stresses vs time for the point on the PDL inner surface at $\varphi = 0$: 1 – $u_0 = 18.15 \cdot 10^{-6}$ (correspond to load of 1 N applied to crown of the tooth root); 2 – $u_0 = 90.75 \cdot 10^{-6}$ (correspond to load of 5 N applied to crown of the tooth root).

2.2. Effect of Poisson's ratio on the normal component of stresses

Frequently used Poisson's ratios, along with 0.49, are 0.30 and 0.45 [1, 22, 23, 24]. Employing of different Poisson's ratios from such large range can significantly affect the results of the finite-element and analytical modelling of the PDL behavior under the static and dynamic loading. So, study [14] has revealed that the instantaneous initial displacement u_0 could change considerably (about to four times) at the change of Poisson's ratio from 0.30 to 0.49. It has been also found that the Poisson's ratio significantly affects stress components, as well as the stresses regimes in the linearly elastic PDL. At the same time, the influence of the Poisson's ratio variation on the time-dependent stresses in the viscoelastic PDL was not analyzed. The patterns of the normal radial stresses in the PDL with Poisson's ratio 0.30, 0.45 and 0.49 at the point of time 2 h are shown in Figure 4. The geometric and other material constants as well as the load were taken as above.

Figure 4 shows that the Poisson's ratio significantly affects both the magnitude of the radial stresses in the PDL and the stress distributions. The lower Poisson's ratio is, the smaller the stresses magnitude becomes. At the same time, decreasing Poisson's ratio leads to increasing the difference between the radial stresses at the inner and outer PDL surfaces. So, for Poisson's ratio $\nu = 0.49$, this difference is 0.7%; for Poisson's ratios $\nu = 0.45$ and $\nu = 0.30$, they are about 3.1% and 9.5%, respectively.

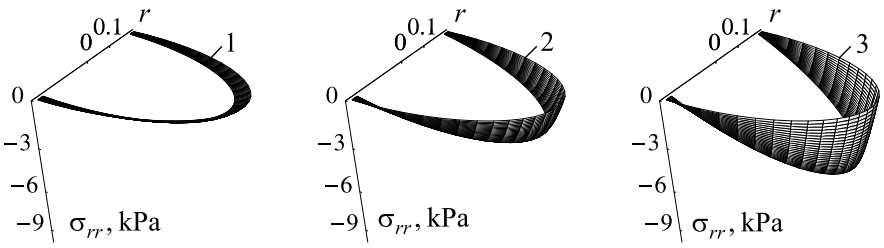

FIGURE 4. Patterns of the normal radial stresses $\sigma_{rr}(r, \varphi, t_3)$ in the PDL for the point of time $t_3 = 2$ h at different values of Poisson's ratio: 1 – $\nu = 0.49$; 2 – $\nu = 0.45$; 3 – $\nu = 0.30$.

3. Conclusions

In this study, the analytical model of the viscoelastic PDL based on fractional viscoelastic model was proposed. It allows to assess the time-dependent stresses in the PDL after the tooth root translational displacement. Parameters for the kernel of relaxation were defined under the assumption that the relaxation of stresses in the PDL tissue occurs in about five hours after definition of the initial displacement of the tooth root. The analysis of performed calculations allows us to make the following conclusions:

- The normal radial and circular components of stresses decrease throughout the thickness of the PDL (from its inner surface to the outer one). Damping of stresses occurs faster for small initial displacement; the larger initial displacement is, the more time for the stress relaxation is required.
- If the PDL is nearly incompressible (with Poisson's ratio $\nu = 0.49$), the normal stresses are changed significantly over the PDL width. The values of Poisson's ratio significantly affects stresses in the PDL tissues. The normal stresses decrease together with Poisson's ratio, the difference between stresses on the inner and outer surfaces of the PDL increasing. Therefore, Poisson ratio may significantly effect on the outcomes of the practical assessment of the PDL behavior based on the linear elastic and viscoelastic models.
- Further development of the proposed model can be associated with the 3-D analytical modeling which would enable to describe the dynamic behavior of the viscoelastic PDL under various loads applied to the tooth root taking into account its real 3-D shape.

The outcomes obtained in this study can be used for simulation of the bone remodelling process during the orthodontic treatment and for assessment of the optimal conditions for the orthodontic load application.

Acknowledgment

This paper is the result of project implementation: TAMER "Trans-Atlantic Micromechanics Evolving Research: Materials containing inhomogeneities of

diverse physical properties, shapes and orientations" supported by FP7-PEOPLE-2013-IRSES Marie Curie Action "International Research Staff Exchange Scheme".

References

[1] T. S. Fill, J. P. Carey, R. W. Toogood, P. W. Major, *Experimentally determined mechanical properties of, and models for, the periodontal ligament: critical review of current literature.* J. Dent. Biomech. (2011) DOI: 10.4061/2011/312980

[2] A. N. Natali, A. R. Ten Cate, *Dental biomechanics.* Taylor and Francis, 2003.

[3] C. Dorow, F. G. Sander, *Development of a model for the simulation of orthodontic load on lower first premolars using the finite element method.* J. Orofacial Orthop. **66** (2005), 208–218.

[4] M. Drolshagen, L. Keilig, I. Hasan, S. Reimann, J. Deschner, K. T. Brinkmann, R. Krause, M. Favino, C. Bourauel, *Development of a novel intraoral measurement device to determine the biomechanical characteristics of the human periodontal ligament.* J. Biomech. **44** (2011), 2136–2143.

[5] F. Groning, M. J. Fagan, P. O'Higins, *The effects of the periodontal ligament on mandibular stiffness: a study combining finite element analysis and geometric morphometrics.* J. Biomech. **44** (2011), 1304–1312.

[6] W. R. Proffit, H. W. Fields, D. M. Sarver, *Contemporary orthodontics.* Mosby, 2012.

[7] W. D. Van Driel, E. J. Van Leewen, J. W. Von den Hoff, J. C. Maltha, A. M. Kuijpers-Jagtman, *Time-dependent mechanical behavior of the periodontal ligament.* Proc. Inst. Mech. Eng. Part H: J. Eng. Med. **214** (2000), 407–504.

[8] C. J. Burstone, R. J. Pryputniewicz, W. W. Bowley, *Holographic measurement of tooth mobility in three dimensions.* J. Periodon. Res. **13** (1978), 283–294.

[9] K. Komatsu, *Mechanical strength and viscoelastic response of the periodontal ligament in relation to structure.* J. Dent. Biomech. (2010) DOI:10.4061/2010/502318

[10] J. Middleton, M. Jones, A. Wilson, *The role of the periodontal ligament in bone modeling: The initial development of a time-dependent finite element model.* Am. J. Orthod. Dentofacial Orthop. **109** (1996), 155–162.

[11] D. C. A. Picton, *Tooth mobility – an update.* Eur. J. Orthod. **12** (1990), 109–115.

[12] L. Qian, M. Todo, Y. Morita, Y. Matsushita, K. Koyano, *Deformation analysis of the periodontium considering the viscoelasticity of the periodontal ligament.* Dent. Mat. **25** (2009), 1285–1292.

[13] S. R. Toms, G. J. Dakin, J. E. Lemons, A. W. Eberhardt, *Quasi-linear viscoelastic behavior of the human periodontal ligament.* J. Biomech. **35** (2002), 1411–1415.

[14] S. Bosiakov, G. Mikhasev, *Mathematical model for analysis of translational displacements of tooth root.* Math. Model. Analysis. **20** (2015), 490–501.

[15] C. G. Provatidis, *An analytical model for stress analysis of a tooth in translation*, Int. J. Eng. Sci. **39** (2001) 1361–1381.

[16] A. Van Schepdael, L. Geris, J. Van der Sloten, *Analytical determination of stress patterns in the periodontal ligament during orthodontic tooth movement.* Med. Eng. Phys. **35** (2013), 403–410.

[17] A. N. Natali, P. G. Pavan, C. Venturato, K. Komatsu, *Constitutive modeling of the non-linear visco-elasticity of the periodontal ligament.* Comp. Meth. Prog. Biomed. **104** (2011), 193–198.

[18] N. Slomka, A.D. Vardimon, A. Gefen, R. Pilo, C. Bourauel, T. Brosh, *Time-Related PDL: Viscoelastic response during initial orthodontic tooth movement of a tooth with functioning interproximal contact – a mathematical model.* J. Biomech. **41** (2008), 1871–1877.

[19] S. Bosiakov, A. Koroleva, S. Rogosin, V. Silberschmidt, *Viscoelasticity of periodontal ligament: an analytical model.* Mech. Adv. Mat. Modern Proc. **1:7** (2015), DOI 10.1186/s40759-015-0007-0

[20] L. Qian, M. Todo, Y. Morita, Y. Matsushita, K. Koyano, *Deformation analysis of the periodontium considering the viscoelasticity of the periodontal ligament.* Dent. Mat. **25** (2009), 1285–1292.

[21] A. Hohmann, C. Kober, P. Young, C. Dorow, M. Geiger, A. Boryor, F. M. Sander, C. Sander, F. G. Sander, *Influence of different modeling strategies for the periodontal ligament on finite element simulation results.* Am. J. Orthod. Dentofacial Orthop. **139** (2011), 775–783.

[22] A. Kawarizadeh, C. Bourauel, A. Jager, *Experimental and numerical determination of initial tooth mobility and material properties of the periodontal ligament in rat molar specimens.* Eur. J. Orthod. **25** (2003), 569–578.

[23] M. Poppe, C. Bourauel, A. Jager, *Determination of the material properties of the human periodontal ligament and the position of the centers of resistance in single-rooted teeth*, J. Orofacial Orthop. **64** (2002), 358–370.

[24] J. S. Rees, P. H. Jacobsen, *Elastic modulus of the periodontal ligament.*, Biomat. **18** (1997), 995–999.

[25] K. Tanne, T. Nagataki, Y. Inoue, M. Sakuda, C. J. Burstone, *Patterns of initial tooth displacements associated with various root lengths and alveolar bone heights.* Am. J. Orthod. Dentofacial Orthop. **100** (1991), 66–71.

[26] K. Tanne, M. Sakuda, C. J. Burstone, *Three-dimensional finite element analysis for stress in the periodontal tissue by orthodontic forces.* Am. J. Orthod. Dentofacial Orthop. **92** (1987), 499–505.

[27] R. F. Viecilli, Th. R. Katona, J. Chen, J. K. (Jr.) Hartsfield, W. E. Roberts, *Three-dimensional mechanical environment of orthodontic tooth movement and root resorption.* Am. J. Orthod. Dentofacial Orthop. **133** (2008), 791.e11–791.e26.

[28] S. A. Wood, D. C. Strait, E. R. Dumont, C. F. Ross, I. R. Grosse, *The effects of modeling simplifications on craniofacial finite element models: The alveoli (tooth sockets) and periodontal ligaments.* J. Biomech. **44** (2011), 1831–1838.

[29] Yu. A. Rossikhin, M. V. Shitikova, *Comparative analysis of viscoelastic models involving fractional derivatives of different orders.* Frac. Calc. Appl. Anal. **10** (2007), 111–121.

[30] Yu. N. Rabotnov, *Equilibrium of an elastic medium with after-effect.* J. Appl. Math. Mech. **12** (1948), 53–62.

[31] Yu. N. Rabotnov, *Elements of Hereditary Solid Mechanics.* Mir Publishers, 1980.

[32] R. Gorenflo, A. Kilbas, F. Mainardi, S. Rogosin, *Mittag-Leffler Functions, Related Topics and Applications.* Springer-Verlag, 2014.

[33] F. Mainardi, *Fractional Calculus and Waves in Linear Viscoelasticity.* Imperial College Press and World Scientific, 2010.

S. Bosiakov
Belarusian State University
4 Nezavisimosti Avenue
Minsk 200030 Belarus
e-mail: bosiakov@bsu.by

G. Mikhasev
Belarusian State University
4 Nezavisimosti Avenue
Minsk 200030 Belarus
e-mail: mikhasev@bsu.by

S. Rogosin
e-mail: rogosin@bsu.by
Belarusian State University
4 Nezavisimosti Avenue
Minsk 200030 Belarus